

Molecular Characteristics of Room-Temperature Soluble Fractions of Low-Density Polyethylene Film Resins

Youlu Yu, Chung C. Tso, Paul J. DesLauriers

Chevron Phillips Chemical Company, LP, Bartlesville Research and Technology Center, Bartlesville, Oklahoma 74004

Received 16 September 2005; accepted 10 November 2005

DOI 10.1002/app.23811

Published online in Wiley InterScience (www.interscience.wiley.com).

ABSTRACT: The molecular characteristics of the room-temperature soluble fractions (RT solubles) of three low-density polyethylene film resins were characterized by size-exclusion chromatography (SEC), SEC combined with FTIR (SEC-FTIR), and nuclear magnetic resonance spectroscopy (NMR). The high-molecular-weight components of the RT solubles were found to be highly branched components with uniform short-chain branching (SCB) profiles. For the low-molecular-weight components, however, SCB content was a function of molecular weight (MW), increasing with an increase in MW. When the chain ends were considered as SCB equivalents, the distribution of the sum of SCB and chain ends across the molecular weight distribution was practically flat, suggesting that the driving force for polymer chains remaining in solution at RT was the length of the undisrupted methylene sequence in the backbone, or methylene run length, which was too short to form crystal lamellae with a melting temperature above RT, regardless of the molecular weight of the polymer. Moreover, the NMR re-

sults revealed that the polymer components of the RT solubles had "superrandom" SCB distributions, that is, the fraction of comonomer clusters in the polymer chains of the RT solubles was lower than that predicted by Bernoullian statistical analysis, indicating that the probability of adding a comonomer to a comonomer-ended propagating chain was lower than that of adding a comonomer to an ethylene-ended one, presumably because of an unfavorable steric effect. Furthermore, contrary to the common belief that RT solubles are mainly low-molecular-weight polymers, high-molecular-weight components were found in high concentrations in the RT solubles, with a cutoff MW as high as 1,000,000 g/mol. The proportion of RT solubles in the film resins was found to depend on the type of resin. © 2006 Wiley Periodicals, Inc. *J Appl Polym Sci* 100: 4992–5006, 2006

Key words: low-density polyethylene; room-temperature solubles; short-chain branching (SCB); molecular characteristics

INTRODUCTION

Components of solutions of ethylene-1-olefin copolymers that do not precipitate or crystallize from the solvent upon cooling to room temperature (RT) are usually called the room-temperature soluble fractions (RT solubles). RT solubles affect polyethylene production, processing, and application in many ways. First, a high RT-soluble content can influence reactor operability and even cause reactor fouling in severe cases.^{1,2} Second, the components of RT solubles are the likely sources of smoking problems during resin processing. And, third, a high RT-soluble content is also a safety concern for polyolefins used in food packaging. Because of this, the FDA strictly limited the content of *n*-hexane extractables,^{3,4} which are believed to be closely related to the proportion of RT solubles in resin. Therefore, an understanding of the molecular characteristics of RT solubles is important in order to control, minimize, and eventually solve RT-soluble-related problems through catalyst technology and/or other engineering means.

Although there has been extensive analysis of hexane extractables of polyethylene (PE), their chemical nature is not fully understood. A literature search revealed no systematic study of the molecular characteristics of the RT solubles of PE film resins, largely because the means to further separate and characterize RT solubles were not available. In the present study, size-exclusion chromatography combined with FTIR (SEC-FTIR) and nuclear magnetic resonance spectroscopy (NMR) were employed to fully characterize the molecular characteristics of the RT-soluble fractions of three low-density film resins: a Cr-catalyst-based low-density linear PE (LDLPE) resin, a conventional Ziegler-Natta-type linear low-density PE (LLDPE) resin, and a metallocene-based LLDPE resin (mLLDPE), all of which are ethylene-1-hexene copolymers of similar densities and fairly similar melt indices. The differences in molecular characteristics of prep-scale and analytic-scale RT solubles also were investigated.

EXPERIMENTAL

Materials

The three parent polymers chosen for this study were low-density polyethylene film resins with fairly simi-

Correspondence to: Y. Yu (yuy@cpchem.com).

lar melt indices and similar densities (0.923, 0.921, and 0.918 g/cm³ for PE-A, PE-B, and PE-C, respectively). Each resin exemplifies a family of Chevron Phillips Chemical (CPChem) polyethylene resins: PE-A is an LDLPE resin made with CPChem's Cr-based catalyst (Phillips catalyst); PE-B, a conventional LLDPE resin made with a Ziegler-Natta-type catalyst; and PE-C, an mLLDPE resin made with CPChem's proprietary metallocene catalyst system.

Extraction of analytic-scale RT solubles

To a suitably sized screw-top bottle (1-oz French square, Fisher Scientific) was added 0.30 g (all weights actual recorded weights) of polyethylene pellets. After adding 14.0 mL of 1,2,4-trichlorobenzene (TCB) solvent containing 0.1% (w/v) 2,6-di-*t*-butyl-4-methylphenol (BHT), the bottle, loosely capped with an aluminum-lined cap, was heated in an air-blowing oven (Blue M, OV-490A-2) at 150°C for 15 min, after which the cap was tightened to avoid excessive oxidation and solvent evaporation. To assist dissolution, the sample bottle was gently rotated periodically and inverted after every other rotation until the polymer was completely dissolved. Then the oven was switched off to allow the solution to naturally cool overnight (measured cooling rate was 0.7–0.9°C/min) to room temperature (RT).

To remove the precipitates from the RT solubles, the slurry in the bottle was filtered using a Whatman Autovial[®] Syringless filter with a pore size of 0.45 μm. The collected filtrate was then transferred to an injection vial for SEC analysis. High-density polyethylene (CPChem Marlex[®] BHB5003) with a broad molecular weight distribution was used as the standard for quantitation. The percentage of RT solubles in a polymer was calculated using the following equation [eq. (1)]:

$$x_{\text{rts}} \% = \frac{A_{\text{unk}} V_{\text{unk}} W_{\text{std}}}{A_{\text{std}} V_{\text{std}} W_{\text{unk}}} \times 100 \quad (1)$$

where $X_{\text{rts}} \%$ is the weight percent (wt %) of RT solubles in the polymer; A , V , and W are the chromatographic area, the volume of solvent used for sample preparation, and the sample weight, respectively; and the subscripts *unk* and *std* are the polymer of interest for RT-soluble analysis and the PE standard, respectively.

Extraction of prep-scale RT solubles

Approximately 15 g of a sample of interest was weighed into a 1-L Erlenmeyer flask to which 800 mL of 1,3,5-trimethylbenzene (TMB) containing 0.1%

(w/v) BHT was subsequently added. The capped flask was then placed in a preheated circulation oven at 130°C for about 12 h, during which occasional agitation was provided to assist the dissolution. The homogeneous solution thus obtained was removed from the oven and left to air-cool to room temperature. After filtering out the precipitate, the filtrate was quickly poured into a 2-gallon glass container that had at least twice as much acetone as filtrate in order to precipitate the RT solubles. The precipitate was collected through filtration, rinsed with acetone, and then dried in a vacuum oven at 40°C until constant weight. The fraction of prep-scale RT solubles was calculated as the ratio of the weight of the recovered RT solubles to that of the parent polymer.

SEC

SEC was performed with a Waters 150-CV or 150-CV+ instrument equipped with a differential refractive index detector and a Waters Styragel HT-6E column set containing two 7.8 × 300 mm columns operated at 140°C with a mobile-phase (TCB) flow rate of 1.0 mL/min. The column set was calibrated against Marlex[®] BHB5003 (CPChem), a high-density PE with a broad molecular weight distribution (MWD), using the integral method.^{6,7} More rigorous calibration using extended low-molecular-weight *n*-alkanes and narrow MWD PE was not pursued in this study.

SEC-FTIR

A detailed description of SEC-FTIR techniques can be found in the literature.⁸ Briefly, solutions of prep- and analytic-scale RT solubles whose concentrations were nominally 0.15% (w/v) were injected into a PL210 SEC/GPC system (Polymer Laboratories) equipped with two PL 20-μm mixed A columns and a flow cell (KBr windows, 1-mm optical path, ca. 30-μL cell volume) through a heated transfer line. A Perkin Elmer model 2000 FTIR spectrometer equipped with a narrow-band mercury cadmium telluride (MCT) detector was employed to obtain the FTIR spectra. Transfer line and flow cell temperatures were kept at 143°C ± 1°C and 140°C ± 1°C, respectively. Chromatograms were generated using root-mean-square absorbance over the 3000–2700 cm⁻¹ spectra. Molecular weight calculations were made using the same broad MWD PE standard. Spectra from of the chromatogram from different elapsed times were subsequently analyzed for comonomer branch levels using chemometric techniques.⁹

NMR

Carbon-13 NMR was carried out with a Varian Unity Inova-500 system running at a C-13 frequency of 125.7

TABLE I
Molecular Characteristics of RT Soluble Fractions and Their Parent Resins

Resin	Total SCB content in parent ^a (mol %)	Total SCB content in RT solubles ^a (mol %)	Analytic RT solubles in parent (wt %)	SCB in RT solubles (wt %)	MW/MWD ^b of parent resins			MW/MWD ^b of analytic RT solubles		
					M_n	M_w	M_w/M_n	M_n	M_w	M_w/M_n
PE-A	3.50 (2.36)	11.3 (6.96)	4.7	15.2	12.0	190	16	1.03 ^c	15.8 ^c	15.3 ^c
PE-B	3.93 (0)	17.7 (0)	7.5	33.8	28.0	126	4.4	12.7 ^c	63.4 ^c	4.99 ^c
PE-C	2.29 (0.12)	nm ^d	0.16	nm ^d	49.0	110	2.2	0.78	0.89	1.2

^a NMR values. Those in parentheses are the butene (or ethyl) content.

^b M_n and M_w are in kilograms per mole.

^c SEC-FTIR results. All other MW/MWD results are from regular SEC.

^d Not measurable and may be treated as essentially zero.

MHz. A PE solution [10% (w/v)] in a solvent containing 90% TCB and 10% of 1,4-dichlorobenzene-d4 (DCB-d4) was placed in a 10-mm Nalorac probe whose temperature was controlled at 125°C. With a sampler spinning rate of 15 Hz, at least 6000 transients were acquired for each solution with the following conditions: acquisition time, 5 s; delay, 10 s; and pulse angle, 90°. By assuming full NOE,¹⁰ these NMR conditions ensured quantitative measurement of all carbon species in the polyethylene chains except for chain ends that had relatively long T_1 values. Peak assignment and SCB quantification were made using the method described by Randall.¹⁰

RESULTS

Molecular characteristics of parent film resins

The basic molecular characteristics of the three resins used in this study are listed in Table I. Figure 1 shows the molecular weight distributions of these three parent resins and their respective short-chain branching distribution (SCBD) profiles, as determined by SEC. As expected, PE-A had the characteristic broad molecular weight distribution (MWD) of a Cr-catalyzed resin, PE-C had the characteristic narrow MWD of a metallocene LLDPE, and the MWD of PE-B was somewhere in the middle. The measured SCBD was typical

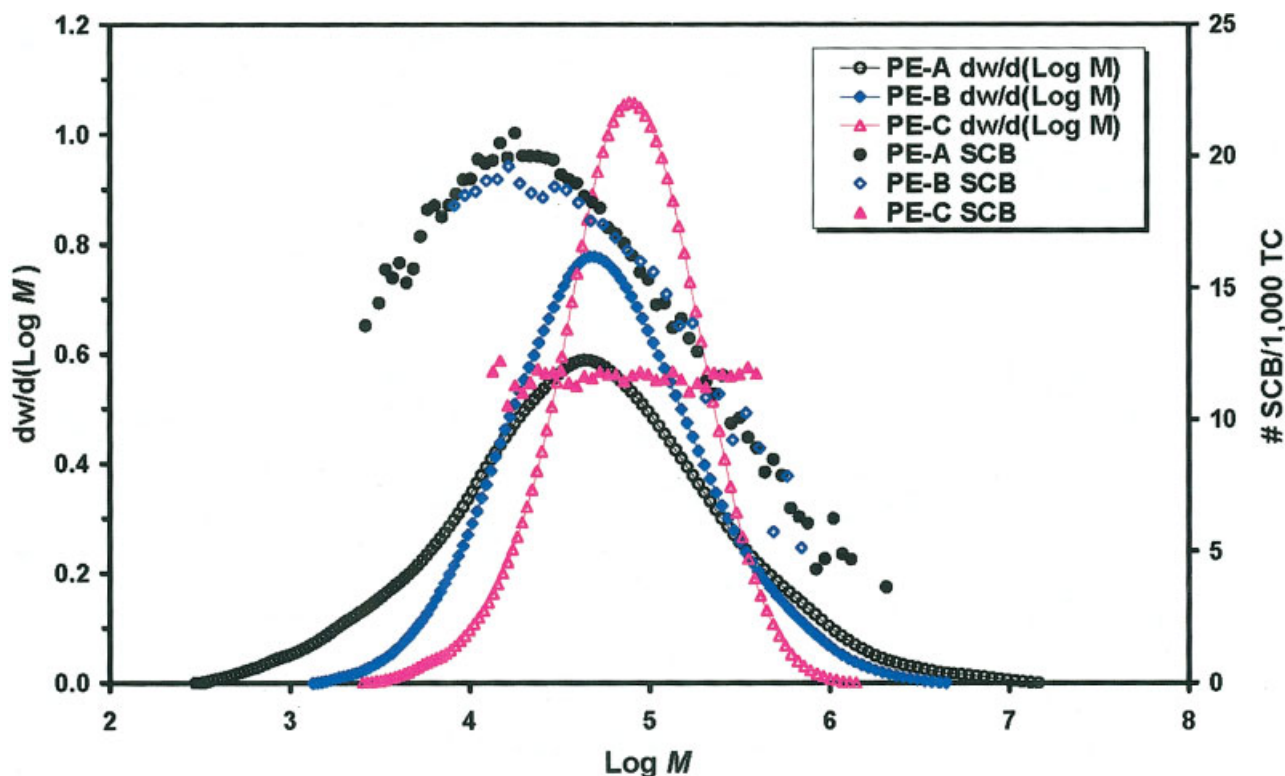


Figure 1 MWD and SCBD profiles of the three low-density resins. [Color figure can be viewed in the online issue, which is available at www.interscience.wiley.com.]

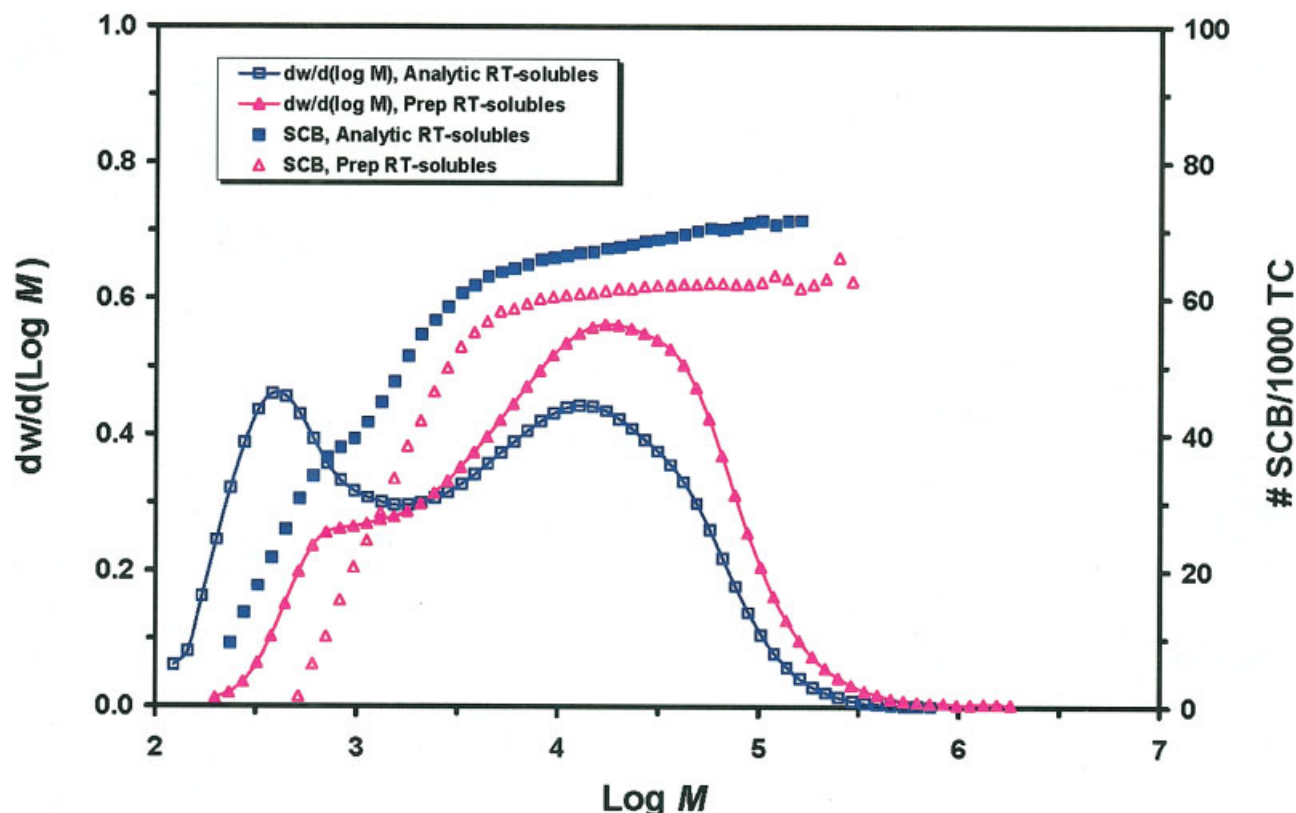


Figure 2 MWD and SCBD profiles of the analytic- and prep-scale RT-soluble fractions of PE-A. [Color figure can be viewed in the online issue, which is available at www.interscience.wiley.com.]

of that reported for these types of polymers, that is, resins made with chromium (PE-A) and Ziegler–Natta (PE-B) exhibited higher comonomer content at the low end of the MWD, whereas that with metallocene catalyst had a flat SCB profile.¹¹ Note that the SCB distributions for PE-A and PE-B were so heterogeneous that at a MW of 10,000 g/mol, the SCB content was almost four times that at a molecular weight of 1,000,000 g/mol.

The three film resins, although very similar in density and melt index, showed dramatically different percentages of RT solubles. As shown in Table I, the level of analytic-scale RT solubles was in the order of PE-B > PE-A ≫ PE-C. Because there was only a trace amount of RT solubles in PE-C, no RT solubles were recovered from the prep-scale extraction.

Molecular characteristics of RT solubles of PE-A

As shown in Figure 2, the MWD profile of the analytic-scale RT solubles of PE-A was distinctively bimodal, with a sharp peak at a MW of about 400 g/mol and another with a relatively broad MWD that peaked at a higher MW of slightly over 10,000 g/mol. With a cutoff MW of about 400,000 g/mol, it was found that for PE-A the total weight percent of analytic-scale RT solubles was 4.7 wt % (Table I). Separate detailed

studies of the same type of resins from different lots found that all their analytic-scale RT solubles had the same distinctive bimodal feature as that shown in Figure 2. However, the total amount of RT solubles varied from lot to lot.

Figure 2 also shows the MWD profile of the prep-scale RT solubles of PE-A for comparison. The major difference between the prep- and analytic-scale RT solubles was that the low-MW peak was significantly reduced in the former. As a result, the bimodal feature of the prep-scale RT solubles fraction was greatly reduced. Concomitantly, the peak MW of the high-MW component and the cutoff MW of the prep-scale RT solubles shifted slightly to the high-MW side. The fraction of prep-scale RT solubles in PE-A also was higher than that of its analytic-scale counterpart (data not shown), presumably because of the different extracting solvents and procedures employed.

SCBD profiles of the analytic- and prep-scale RT solubles superimposed, shown in Figure 2, indicate that at low molecular weight, both the analytic- and prep-scale RT solubles contained a very low level of SCB. However, SCB content increased rapidly as the MW increased up to an MW of about 4500 g/mol. From that point, very little change in the SCB level was observed with increases in MW, that is, the SCB content almost leveled off after the MW exceeded 4500

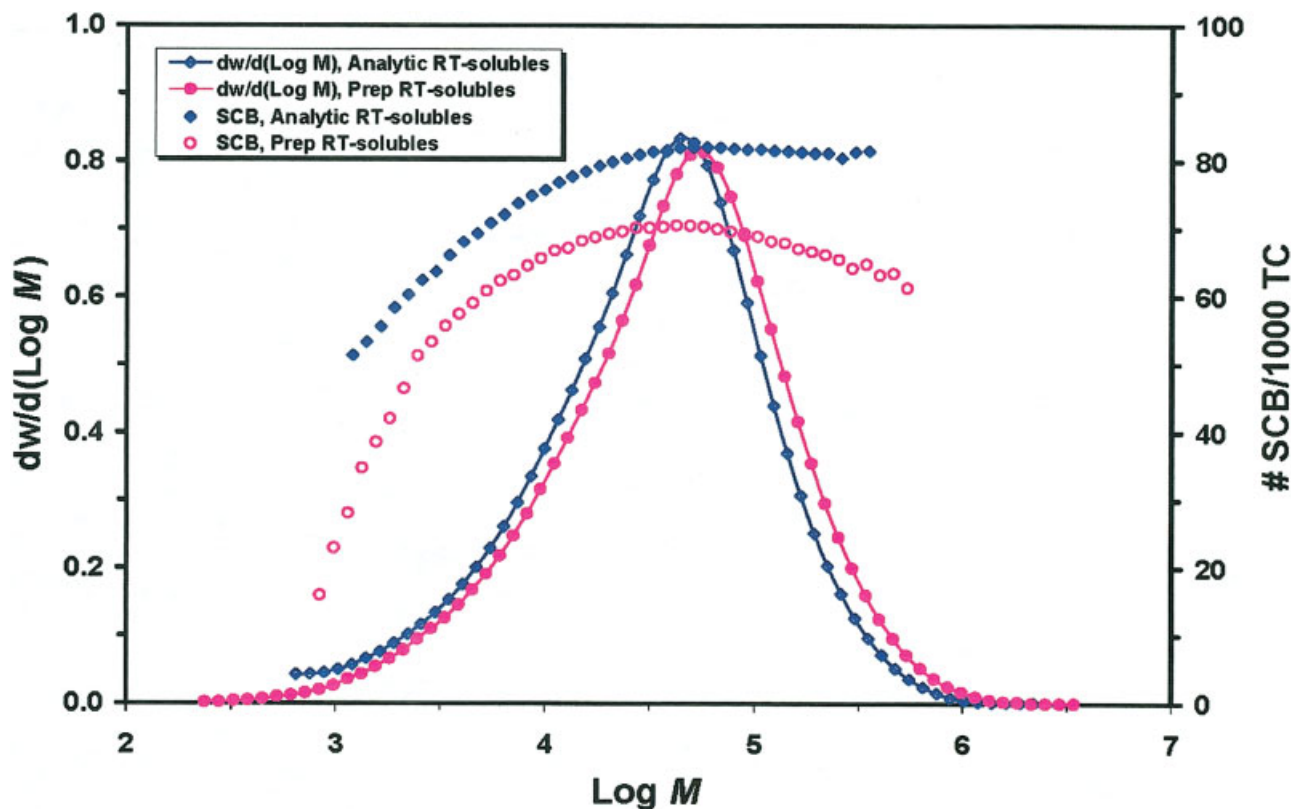


Figure 3 MWD and SCBD profiles of the analytic- and prep-scale RT-soluble fractions of PE-B. [Color figure can be viewed in the online issue, which is available at www.interscience.wiley.com.]

g/mol. In this nearly flattened region, the average SCB content of the analytic-scale RT solubles was 68/1000 total carbons (TC), 6 more than the SCB content of the prep-scale RT solubles of 62/1000 TC. It seemed that in order for high-molecular-weight PE molecules not to precipitate from TCB at room temperature, the RT solubles had to have a high enough SCB content to interrupt the chain regularity such that either the polymer chains were uncrystallizable or the melting temperature of the crystals was at or below room temperature (see the Discussion section).

A comparison of the SCBD profile of the analytic-scale RT solubles with that of the prep-scale RT solubles suggested that the missing components of the prep-scale sample were those that were both low in molecular weight and had a high level of branching. Fractions with low MW and low SCB content could still be precipitated and recovered in the prep-scale RT solubles.

Molecular characteristics of RT solubles of PE-B

Figure 3 shows the MWD profiles of the analytic- and prep-scale RT solubles of PE-B, indicating both to be single modal. Although the analytic-scale RT-soluble sample had a slightly higher weight-average molecular weight (M_w) than did the prep-scale sample, it had

virtually the same cutoff MW as the prep-scale sample. The cutoff MW for all PE-B RT solubles was at least 1,000,000 g/mol. The total weight percent of analytic-scale RT solubles in PE-B was found to be 7.5 wt %, which, as expected, was less than that of the prep-scale RT solubles.

The SCBD profiles of the analytic- and prep-scale RT solubles of PE-B, presented in Figure 3, showed a similar trend, that is, SCB content increased rapidly as the molecular weight increased until the molecular weight reached about 20,000 g/mol. After that, the SCB content marginally increased or decreased as a function of the molecular weight. In this uniform region, the average SCB content of the analytic- and prep-scale RT solubles was 82 and 67/1000 TC, respectively. As with PE-A, the SCB content of the analytic-scale RT solubles was 15/1000 TC greater than that of the prep-scale RT solubles in this region. Again, these differences between the analytic- and prep-scale RT solubles in the total amount of RT solubles, MW/MWD, and SCBD presumably resulted from the use of different solvents and procedures to extract the RT solubles.

Molecular characteristics of RT solubles of PE-C

In contrast, the molecular characteristics of the RT solubles of PE-C were dramatically different from

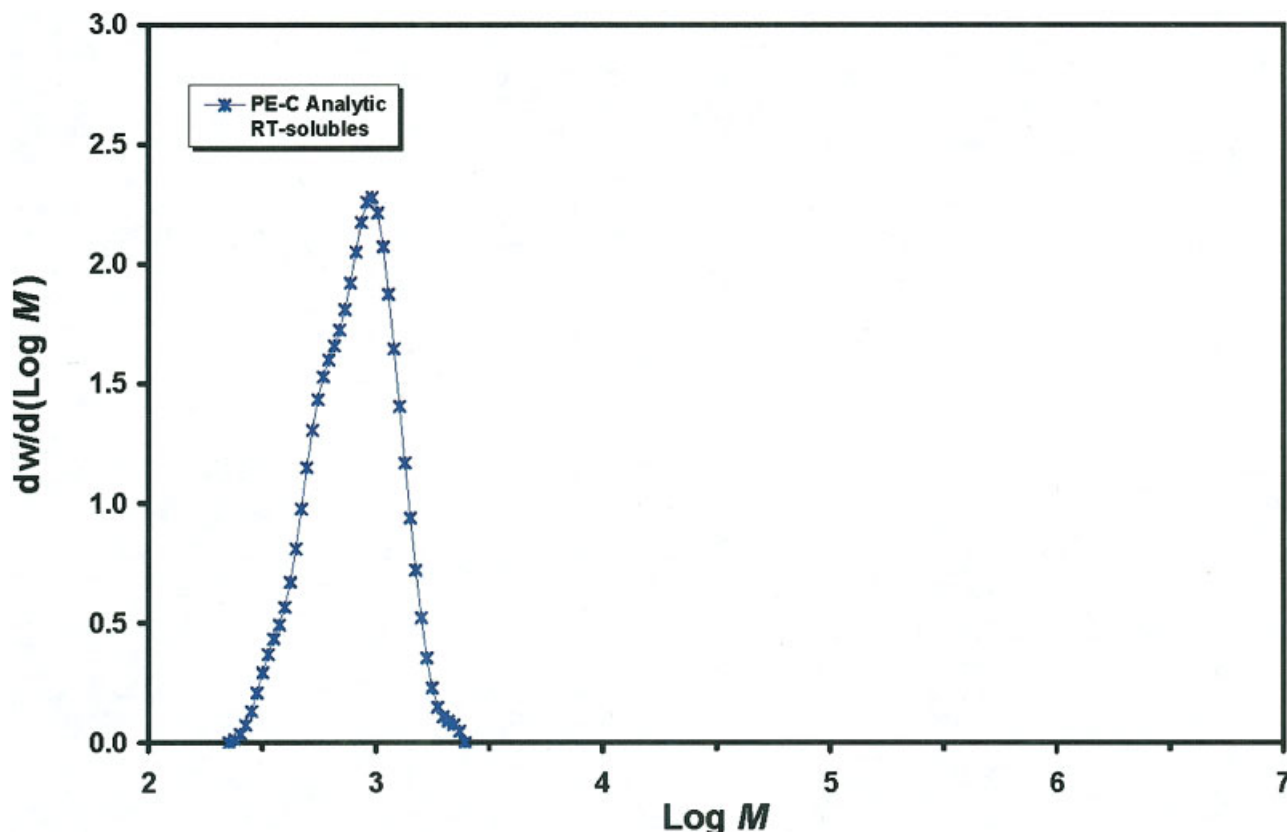


Figure 4 MWD profile of analytic-scale RT solubles of PE-C. [Color figure can be viewed in the online issue, which is available at www.interscience.wiley.com.]

those of PE-A and PE-B. First, PE-C contained a much smaller percentage of RT solubles than did PE-A and PE-B (Table I). The RT-soluble fraction was so small in PE-C that no RT solubles were recovered from the prep-scale extraction. Second, as shown in Table I and Figure 4, the average molecular weight of the analytic-scale RT solubles of PE-C was very low and the MWD extremely narrow ($M_w/M_n = 1.13$).

Because the solution concentration of analytic-scale RT solubles prepared using the extraction method described in the Experimental section was below the detection limit of SEC-FTIR, the concentrations of the RT solubles had to be increased in order to have decent S/N for FTIR signals that would be suitable for SCB calculation. To increase the concentration of RT solubles, the filtrate from a previous run was reused as the solvent in another extraction and so forth until the S/N of the FTIR signal was good enough for the calculation. However, the FTIR spectra of the RT solubles thus obtained suggested that most components of the RT solubles of PE-C were nonpolyethylene materials because the extracts seemed to possess the spectral characteristics of resin additives. Consequently, using the chemometric method, the solution of RT solubles of PE-C was treated as an outlier.⁹

Comparison of RT solubles between PE-A with PE-B

Figure 5 compares the molecular characteristics of analytic-scale RT solubles of PE-A with those of PE-B. First, it shows that they had very different MWD profiles, with the MWD of the RT solubles of PE-A being distinctively bimodal, but that of PE-B having a single, rather symmetrical mode and a much higher weight-average molecular weight. Second, the comparison shows a considerable difference between the RT solubles of PE-A and of PE-B in SCB content. Noticeably, the SCB content of the sample of RT solubles of PE-B was, on average, about 14 SCB/1000 TC higher than that of PE-A at the same molecular weight. And, third, the comparison shows that at the high end of the MWD, the RT solubles of PE-B had a larger cutoff molecular weight than did those of PE-A. Because the parent polymers, PE-A and PE-B, had nearly identical SCBD profiles (Fig. 1), these results indicate that PE-B was more inter- and/or intramolecularly heterogeneous than was PE-A. Similar differences in molecular characteristic were found between the prep-scale RT solubles of PE-A and those of PE-B, but to a lesser extent (see Fig. 6).

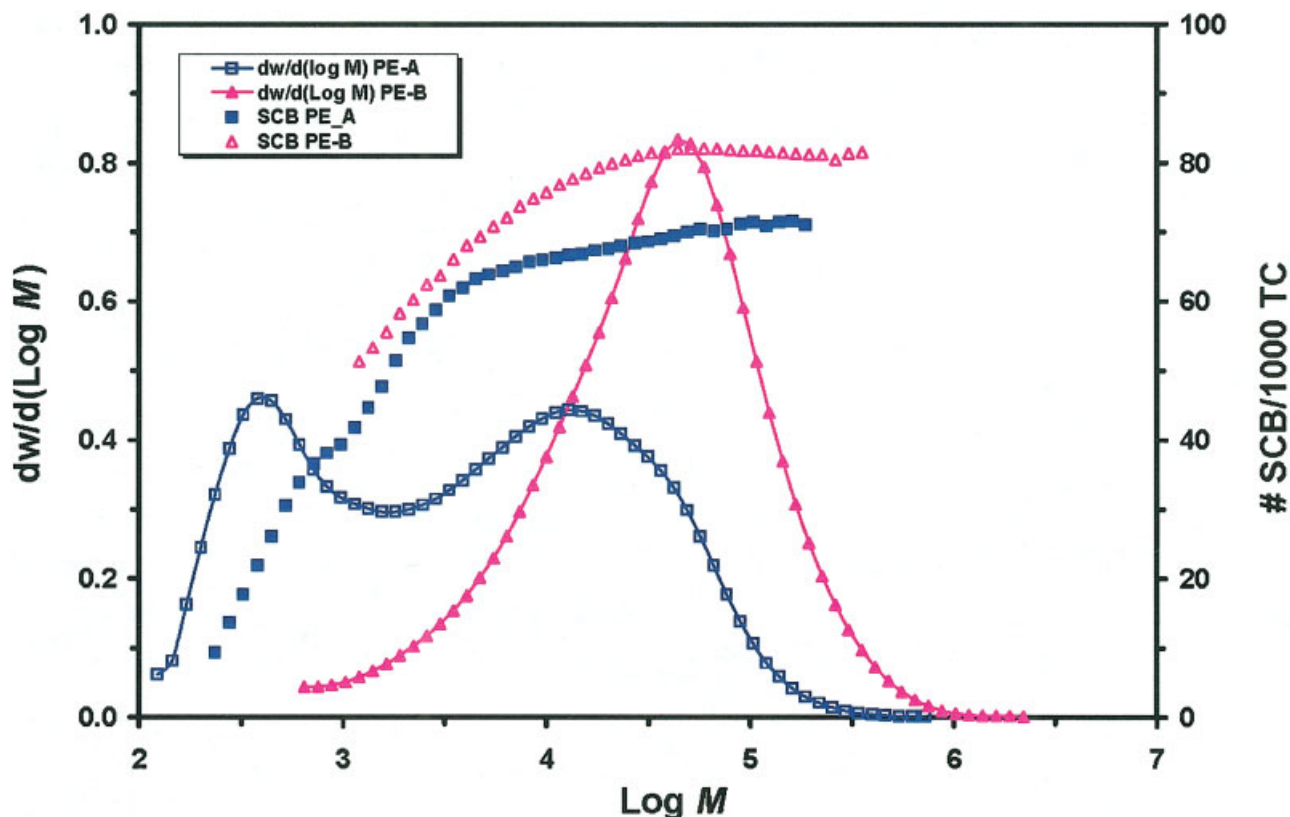


Figure 5 MWD and SCBD profiles of the analytic-scale RT solubles of PE-A and PE-B. [Color figure can be viewed in the online issue, which is available at www.interscience.wiley.com.]

Comparison of MWD profiles of parent polymers with their RT solubles

Presented in Figures 7–9 are the MWD profiles of PE-A, PE-B, and PE-C, respectively, together with the weighted profiles of the corresponding analytic-scale RT solubles, weighted according to the weight percent of the respective full polymer (Table I). For the profile of the very small RT-soluble fraction of PE-C (Fig. 9), the y axis value had to be multiplied by a factor of 5 in order to be clearly visible (Fig. 9). A comparison of the MWD profile of the RT solubles of PE-A with that of the parent polymer indicated that, although the weight-average molecular weight of the RT-soluble fraction was much smaller than that of its parent resin, its polydispersity (M_w/M_n) was similar. This is because the solvent extracted almost all the RT-solubles of the low MW tail ($MW \leq 1000$ g/mol) of PE-A from the parent (Fig. 7). Furthermore, although polymers with a MW larger than 300,000 g/mol were a sizable fraction of the parent polymer, no RT solubles of MW 300,000 g/mol or higher were extracted, indicating that the RT-soluble fraction was not simply proportional to the population of parent polymers of the same molecular weight, but rather was proportional to SCB heterogeneity in each fraction of the molecular weight of the polymer.

By the same token, a comparison of the MWD profiles of the RT-soluble fraction of PE-B with that of the parent polymer showed that the population of the RT solubles seemed to be proportional to that of the parent at the same MW (Fig. 8), which was significantly different from the results for PE-A discussed above. In summary, we found that (1) the cutoff MW of the RT solubles of PE-B was closer to that of its parent; (2) most of the components of the RT solubles had molecular weights greater than 10,000 g/mol; (3) the peak molecular weight of the RT solubles was close to that of its parent; and (4) as pointed out above, components of the RT solubles of PE-B had molecular weights exceeding 1,000,000 g/mol. Albeit the relative amount of RT insolubles at the low MW was higher than that at the high MW presumably because of the chain-end effect (*vide infra*), the relatively higher population of RT solubles at the high molecular weight shown in Figure 8 compared to that shown in Figure 7 again suggests that the inter-/intra-chain heterogeneity in PE-B was higher than that in PE-A.

Unlike with PE-A and PE-B, the MWD profiles of the PE-C parent overlaying its RT solubles indicated little overlap in molecular weight (Fig. 9). This strongly suggests that the extracted RT solubles were materials foreign to the parent polymer, such as poly-

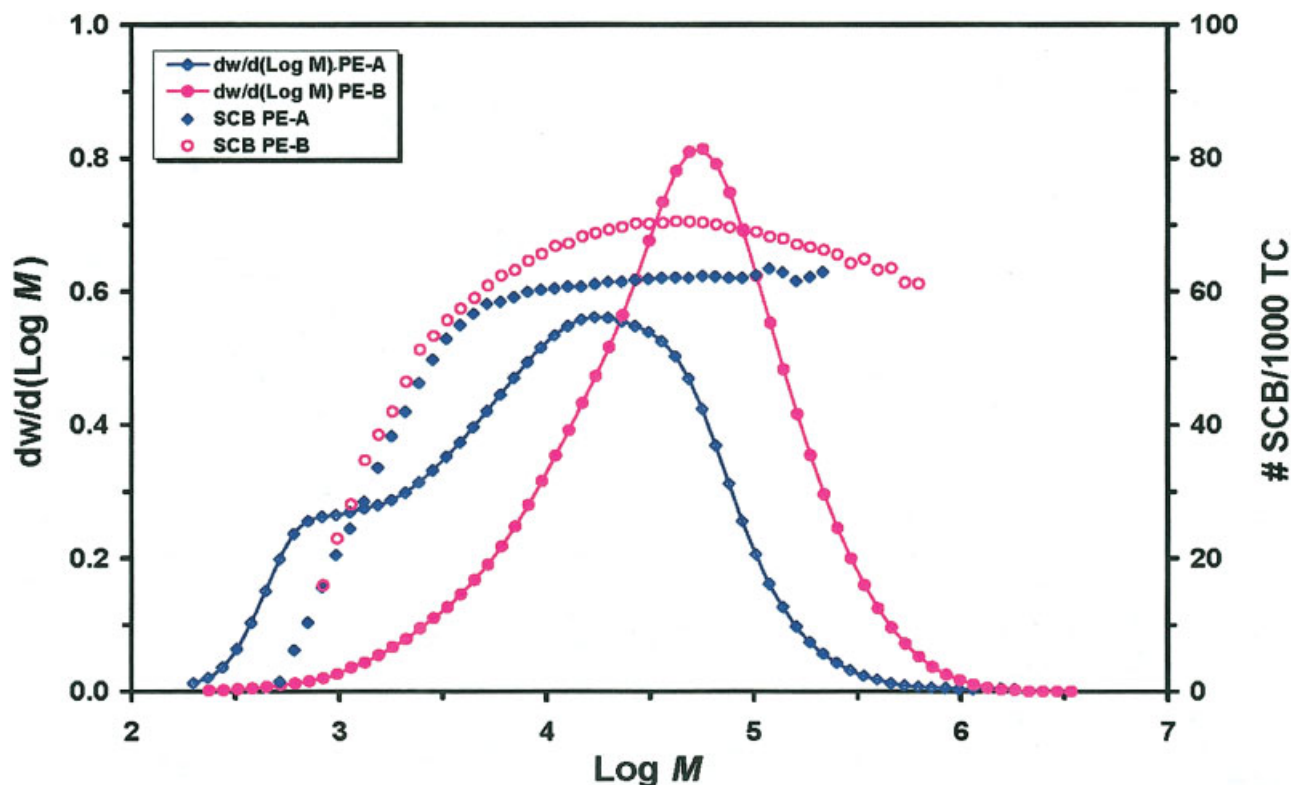


Figure 6 MWD and SCBD profiles of the prep-scale RT solubles of PE-A and PE-B. [Color figure can be viewed in the online issue, which is available at www.interscience.wiley.com.]

mer additives, in keeping with the FTIR results discussed above.

Comonomer dispersion in RT solubles

Shown in Table II are the NMR results for the RT solubles. In addition to the diad and triad distributions, relative monomer dispersion (RMD) and clustering index^{10,12} also are listed in Table II. RMD is the ratio of the measured monomer dispersion to the random Bernoullian distribution.^{13,14} The clustering index, on the other hand, is a measure of the blocked comonomer units in an ethylene-1-olefin copolymer relative to the Bernoullian distribution as the reference point. The clustering index was defined by the eq. (2)^{10,12}:

$$\text{Clustering Index} = 10 \left[1 - \frac{[EXE]_{\text{obs}} - [EXE]_{\text{Bern.}}}{[X] - [EXE]_{\text{Bern.}}} \right] \quad (2)$$

where $[EXE]_{\text{obs}}$ and $[EXE]_{\text{Bern}}$ are the observed and Bernoullian $[EXE]$, respectively. If there was no clustering on the chain, the clustering index should have been zero, resulting in the observed $[EXE]$ being equal to $[X]$. In such cases, the propagating chain with a comonomer at the chain end would reject incorpora-

tion of another comonomer. On the other hand, when the SCBs were randomly distributed across the polymer chain, as predicted by Bernoullian statistical analysis, the clustering index was 10, that is, the observed $[EXE]$ equaled the Bernoullian $[EXE]$. A clustering index larger than 10 indicates more comonomer clustering on the polymer chain than predicted by the Bernoullian statistics.

The RMD and clustering index values shown in Table II both seem to indicate that the comonomer in the RT solubles of both PE-A and PE-B was superrandomly distributed across the polymer chain, that is, the observed comonomer clustering was lower than that predicted by the Bernoullian statistics. As a result, the RMD for the RT solubles of both polymers was larger than 100, and the clustering index was less than 10. These results are very interesting and suggest that copolymers in the RT solubles with such high SCB content (Table I) would still show comonomer-rejecting behavior during the polymerization process.

DISCUSSION

Chemical nature of RT solubles

Contrary to the common belief that RT solubles are mostly very low-molecular-weight polymers, a large population of polymers in the RT solubles of PE-A and

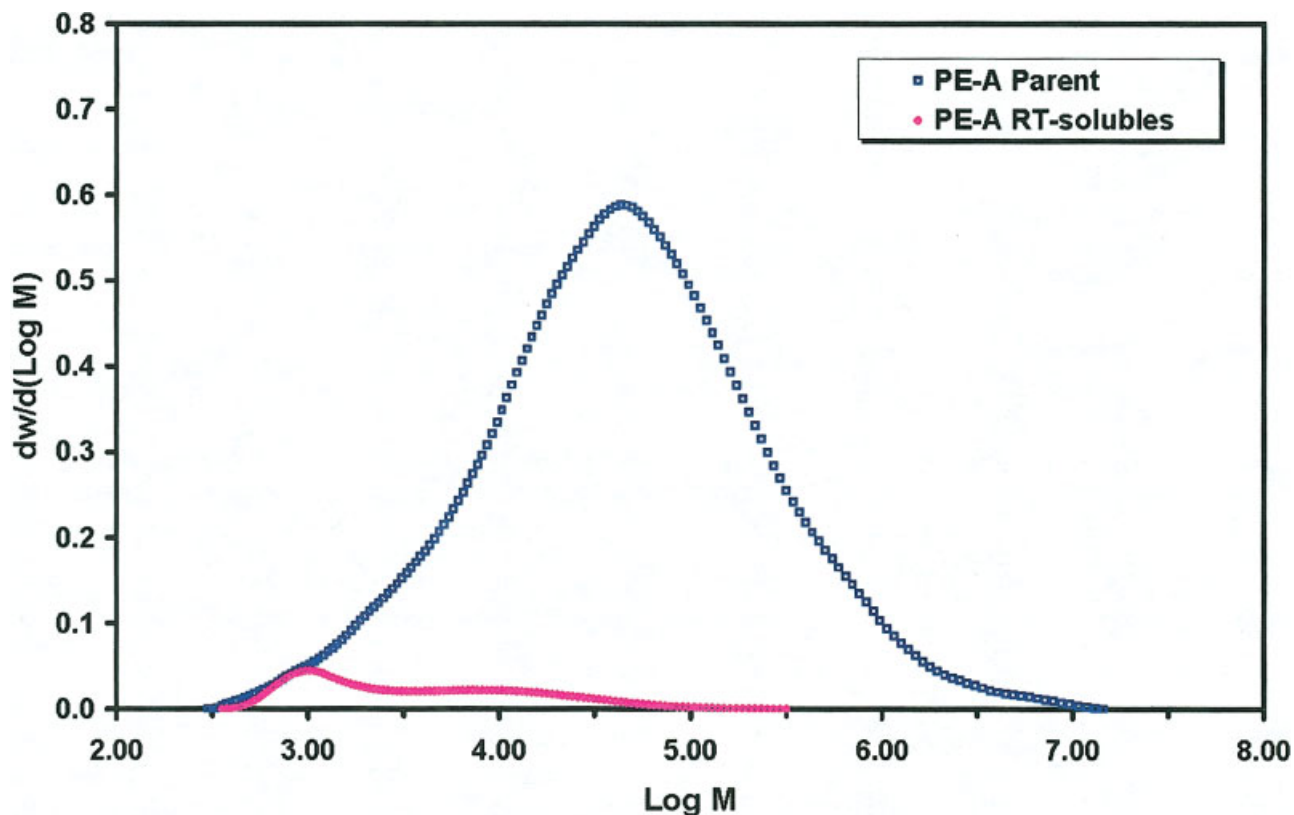


Figure 7 MWD profile of PE-A overlaying weighted MWD profile of its RT solubles (weighted according to weight percent). [Color figure can be viewed in the online issue, which is available at www.interscience.wiley.com.]

PE-B had molecular weights greater than 10,000 g/mol (Figs. 2 and 3). Polymers with MWs higher than 100,000 g/mol of various types also were found in the RT solubles of both PE-A and PE-B. Now the questions are: why do such high-molecular-weight polymers stay dissolved on cooling to room temperature, and what prevents a polymer chain of such high MW from crystallizing/precipitating from the solvent at the RT?

Fundamentally, for a PE chain to remain in the solution at RT, the polymer chain must be either uncrystallizable because of chain irregularity or crystallizable below RT. It is well established that the melting temperature of a crystalline polymer is directly related to the lamellar thickness of the crystalline phase of the polymer, as described by eq. (3)^{15,16}:

$$T_m(l_c) = T_m^0 \left(1 - \frac{2\sigma_e}{\Delta H l_c} \right) \quad (3)$$

where T_m and T_m^0 are the melting and equilibrium melting temperatures, respectively; σ_e is the crystal surface free energy; ΔH is the heat of fusion; and l_c is the lamellar thickness. Among other factors, lamellar thickness is mainly determined by the length of the undisrupted sequence of the repeating units (in this case, $-\text{CH}_2-$), or run length, of the polymer.

For a PE copolymer of the general chemical formula:



where R is the residual alkyl group from the comonomer (a butyl group for an ethylene-1-hexene copolymer, an ethyl group for an ethylene-1-butene copolymer, and so on), M is the molecular weight, x_{SCB} is the short-chain branching content, (number of SCB/1000 TC), and l_r is the run length of the methylene group, $-\text{CH}_2-$, have the following relationships:

$$M = mM_1^0 + nM_2^0 \quad (5)$$

$$x_{\text{SCB}} = 1000*n/(2m + \kappa n) \quad (6)$$

$$l_r = (2m/n) + 1 \quad (7)$$

where m and n are the numbers of ethylene and comonomer units, respectively, in a polymer; and M_1^0 and M_2^0 are the unit molecular weights of ethylene and of the comonomer, respectively; and κ is the number of carbons in the comonomer (if the comonomer is 1-hexene, κ is 6, and so on).

Note that chain ends were neglected. That is because for large-molecular-weight polymers, the weight percent of the polymer chain ends was so small

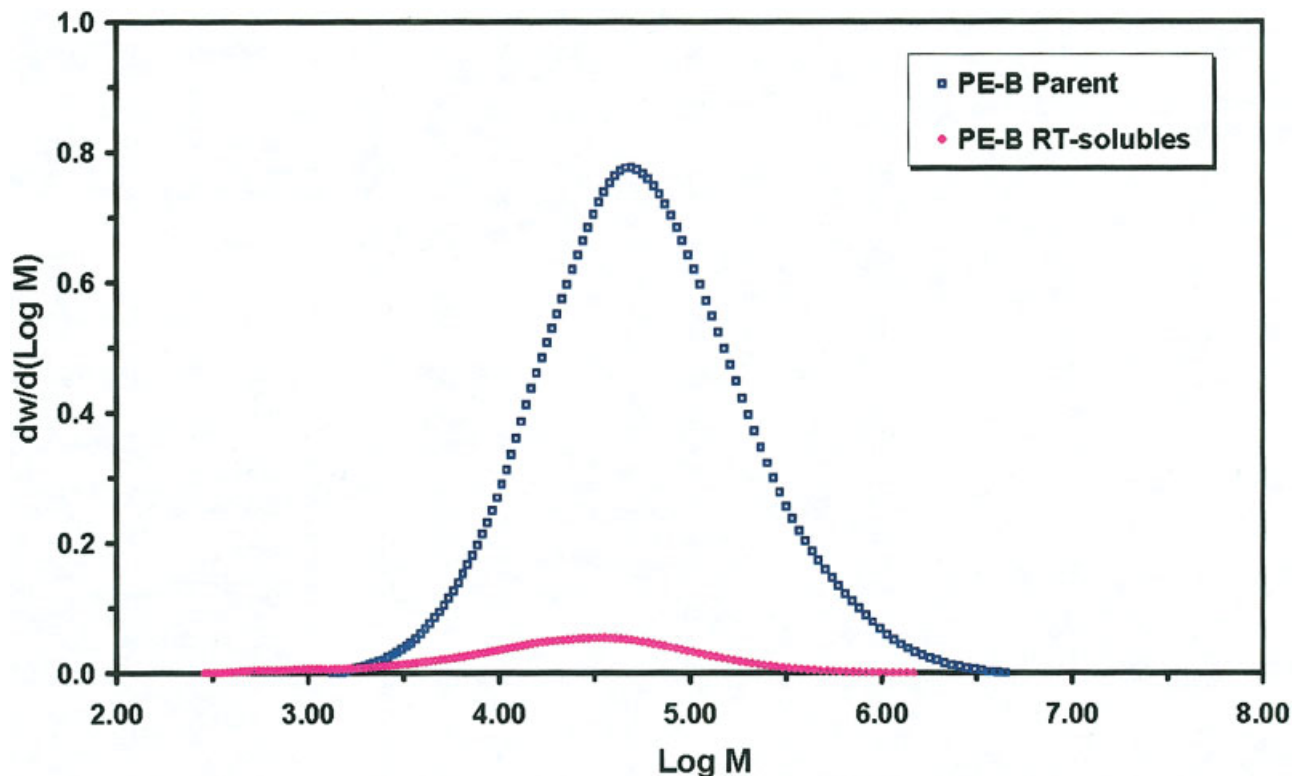


Figure 8 MWD profile of PE-B overlaying weighted MWD profile of its RT solubles (weighted according to weight percent). [Color figure can be viewed in the online issue, which is available at www.interscience.wiley.com.]

that approximating it did not result in any significant error. However, for low-molecular-weight polymers, the weight percent of the polymer chain ends in the polymer was large enough that the chain-end effect could no longer be neglected.

The number of chain ends, x_{CE} (number of chain ends/1000 TC), can be calculated, assuming both chain ends are methyl, with eq. (8):

$$x_{CE} = 1000 \cdot 2 / (2m + \kappa n + 2) \quad (8)$$

where the 2 in the numerator and the denominator means that each polymer molecule has two chain ends. Similar calculations can be done with other types of chain ends. Eq. (8) clearly indicates that x_{CE} was inversely proportional to the molecular weight, that is, the higher the M , the smaller the x_{CE} .

Using eqs. (5)–(7), the methylene run length can be calculated for a copolymer of a given SCB content and molecular weight. For example, as shown in Figure 2, the average SCB content in the high-molecular-weight region of the analytic-scale RT solubles was 68 SCB/1000 TC, which translates as an average methylene run length of about 10. This means that for every 10 —CH₂— repeating units, there would be a comonomer moiety to disrupt the regularity of the chain. The average methylene run lengths of all the RT-soluble fractions in the flat region are listed in Table III. De-

pending on the polymer and extraction procedures, the average run length was near 10. Under comparable conditions, the run length of the RT solubles of PE-A was longer than that of PE-B. And the run length of the prep-scale RT solubles was longer than that of the analytic-scale RT solubles.

Plotted in Figure 10 is the relationship between melting temperature and reciprocal molecular weight of the low-molecular-weight *n*-alkanes.¹⁷ Because *n*-alkanes are low-MW ethylene homopolymer analogs, the relationship between chain length and melting temperature of the *n*-alkanes may shed light on understanding the chemical nature of the RT solubles. Just as predicted by eqs. (3) and (7), a nice linear relationship was obtained for the *n*-alkanes, shown in Figure 10. It is especially interesting that although *n*-hexadecane [CH₃(CH₂)₁₄CH₃] is a liquid at room temperature, meaning its melting point is below room temperature, *n*-octadecane [CH₃(CH₂)₁₆CH₃], on the other hand, is a solid at room temperature, with a melting temperature well above RT (28°C–30°C). Given that the chain ends were excluded and could not be incorporated into the crystal lattice of *n*-alkane and assuming that four carbons from each end of *n*-octadecane molecule were excluded from the crystal lattice, the run length of an *n*-octadecane molecule became 10 methylene groups, which was in good

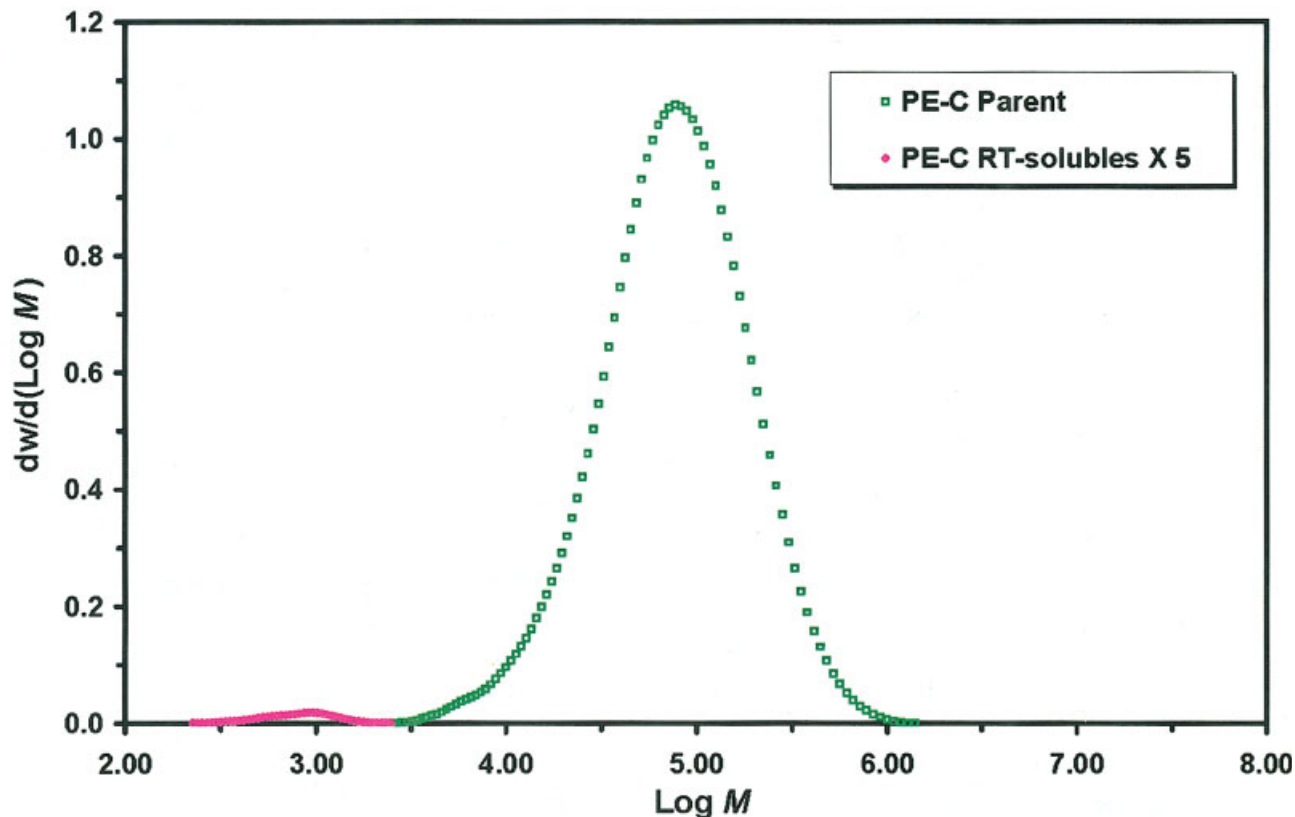


Figure 9 MWD profile of PE-C overlaying weighted MWD profile of its RT solubles (weighted according to weight percent). [Color figure can be viewed in the online issue, which is available at www.interscience.wiley.com.]

agreement with the run length determined for the RT solubles in the nearly flat regions, as shown in Table III. Because TCB is a good solvent for PE, as long as the PE has no crystallinity, it will be soluble in TCB. This suggests that the driving force keeping the RT solubles in solution at room temperature was methylene run length, which was so short for these RT solubles that if any crystals formed, they would have melting temperatures at or below room temperature.

However, the components of the low-molecular-weight region of the RT solubles, shown in Figures 2 and 3, had a lower SCB content, which was also a

function of the molecular weight. At first glance, this suggests that the run length of the low-MW components of the RT solubles would be longer than that of the high-MW components. But this was not the case when the chain ends were considered. Presented in Figure 11 is the distribution profile of the sum of SCB and chain ends across the MWD, with each chain end counted as the equivalent of 1 SCB. For comparison, Figure 11 also shows the normal SCBD. It is clear that when the chain ends were considered, the sum of the SCB and the chain ends, within the experimental error, became almost independent of the molecular weight

TABLE II
Results of NMR Analysis of RT-Soluble Fractions

Sample	Diad distribution ^a			Triad Distribution ^a						RMD ^b (%)	Clustering index ¹⁰
	[EE]	[XE]	[XX]	[EEE]	[XEE]	[XEX]	[EXE]	[XXE]	[XXX]		
PE-A	0.7767	0.2200	0.0032	0.6793	0.1949	0.0125	0.1080	0.0041	0.0012	109.5	2.2
PE-B	0.6725	0.3016	0.0259	0.5569	0.2312	0.0352	0.1330	0.0356	0.0061	103.8	7.7
PE-C	na ^c	na ^c	na ^c	na ^c	na ^c	na ^c	na ^c	na ^c	na ^c	na ^c	na ^c

^a E and X stand for ethylene and the comonomer(s), respectively. The concentration of an *n*-ad is the total concentrations of all *n*-ads in the same category. For example, [XXE] is the sum of [HHE], [BHE], [HBE], and [BBE] for polymers having both ethyl and butyl branches.

^b Relative monomer distribution (RMD), which is defined as the Bernoulli monomer dispersity divided by the observed monomer dispersity, as determined by NMR.^{10,11} See text for detail.

^c Not available.

TABLE III
SCB Content and Corresponding Methylene Run Length
in the Flat SCBD Regions of RT Solubles

	Analytic-scale RT solubles		Prep-scale RT solubles	
	$x_{\text{SCB}}^{\text{b}}$	Run length	$x_{\text{SCB}}^{\text{b}}$	Run length
PE-A ^a	68	9.7	62	11.0
PE-B	82	7.2	67	9.9

^a Resin contains a large amount of *in situ* ethyl branches, the amount of which is given in Table I. For the same total SCB content (SCB/1 000 TC) the run length of this polymer should be longer than the ethylene-1-hexene copolymer PE-B at the same molecular weight.

^b A Mean value.

except at very low molecular weights ($MW < 1000$ g/mol), where the sum of the SCB and the chain ends seemed to increase as the molecular weight decreased. This curvature was likely a result of inaccuracy in the determined MW values because, according to eq. (8), normal errors in MW can result in significant errors in x_{CE} for very low-MW components ($MW < 1000$ g/mol). Therefore, the data presented in Figure 11 are in line with the above conclusion, that is, it is run length that determines if a polymer remains in or precipitates from a solvent.

It is interesting that the SCB content in the flat region of the RT solubles of PE-A was lower than that of PE-B. The heterogeneity of the SCB distribution in polymer chains seems to play a role in this. As shown in Table II, both the RMD values and the clustering indices indicated that the comonomer in the RT solubles of both PE-A and PE-B was superrandomly distributed across the polymer chain because both polymers had an RMD larger than 100 and a clustering index less than 10. In other words, the dispersion of the comonomer in the RT solubles was higher than the Bernoullian random distribution. These very interesting results seem counterintuitive because polymers with such high SCB content (Table I) still showed comonomer-rejecting behavior. But this actually makes sense because polymers containing clustered bulky comonomer sequences would be involved in higher steric energies rather than those having randomly or superrandomly distributed bulky groups at the same given comonomer content, although for copolymers containing a very small amount of SCB, the probability of one comonomer being adjacent to another was so low that the monomer sequence distribution appeared to be random and unselective.¹² For the RT solubles that had a very high SCB content (Table II), on the other hand, the observed number of

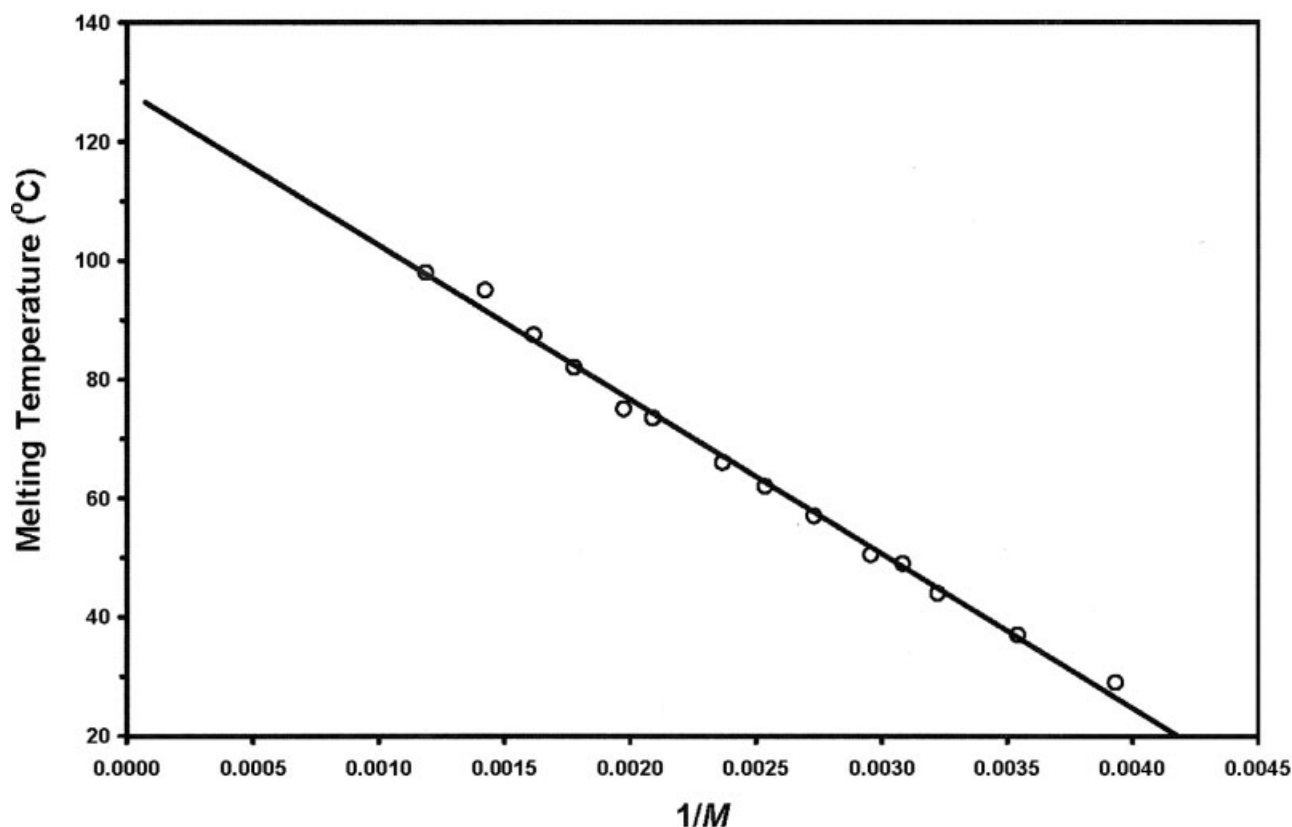


Figure 10 Melting temperature as a function of reciprocal of molecular weight for normal alkanes. The melting temperature data taken from Aldrich Chemical Company Catalog.¹⁷

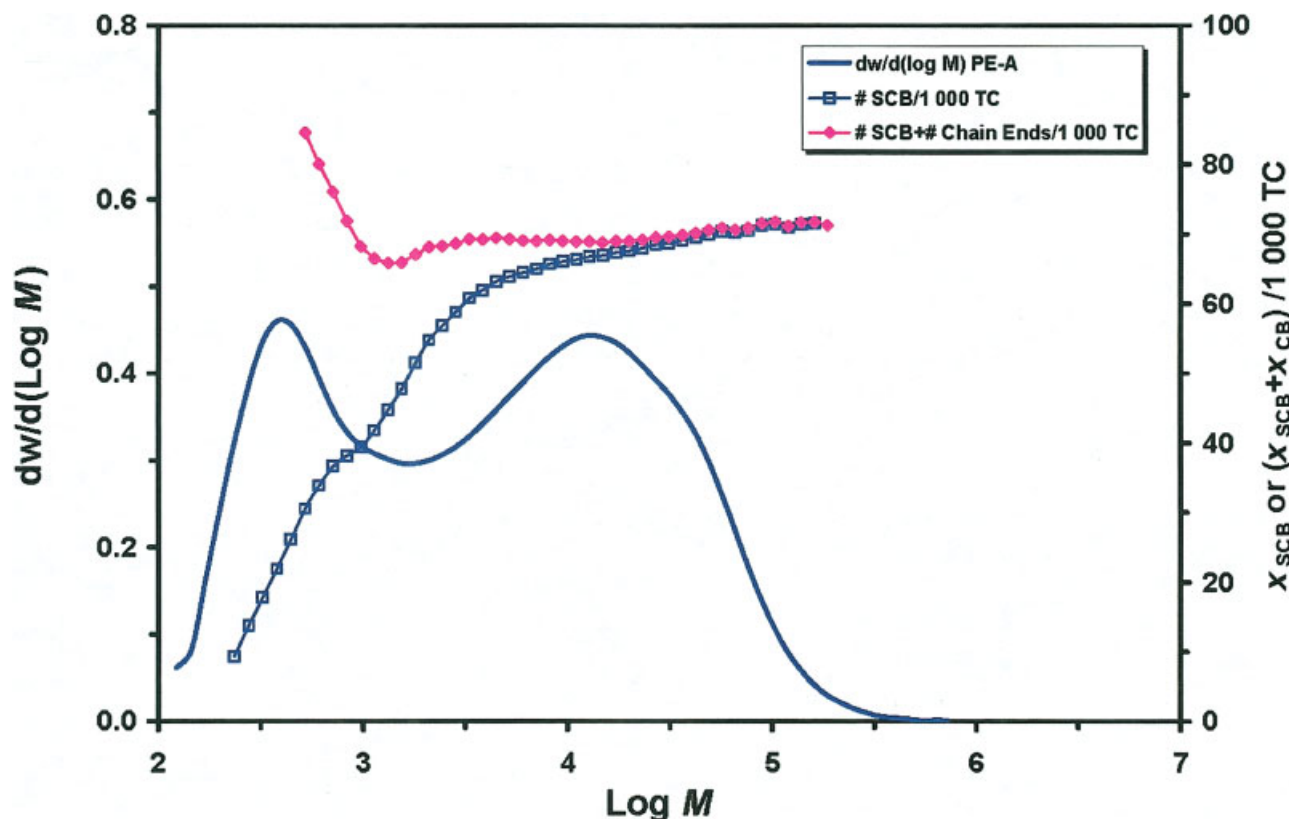


Figure 11 Sum of SCB and chain ends as a function of molecular weight, with each chain end treated as the equivalent of 1 SCB. [Color figure can be viewed in the online issue, which is available at www.interscience.wiley.com.]

comonomer clusters was clearly lower than expected by the Bernoullian statistics, indicating selectivity for the propagating chain ends to add the next monomers. The addition of a bulky comonomer adjacent to a bulky comonomer at the propagating chain end involved higher steric energy than did the addition of a less bulky ethylene unit. Consequently, this would result in a superrandomly distributed SCB across the polymer chains, in keeping with the experimental results.

The clustering index of the RT solubles of PE-B was higher than that of PE-A, 7.7 versus 2.2 (Table II), suggesting that the SCB distribution in the RT solubles of PE-A was more random than that in the RT solubles of PE-B. As a result, for the same average SCB content, the run length of some segments of the RT solubles of PE-B could be longer than that of PE-A despite having the same average run length. It is also possible that the RT solubles of PE-B had higher intermolecular heterogeneity than did the RT solubles of PE-A.

Hosoda studied the extraction temperature of TREF fraction as a function of its SCB content for LLDPE.¹⁸ Figure 12 plots the data from that study,¹⁸ where trend lines 1 and 2 are linear regression lines with and without the highest SCB content data point. The predicted SCB content of the RT extractables was 48 and 52 SCB/1000 TC from trend lines

1 and 2, respectively. The latter number is more likely to be reliable because very highly branched PE may not reach its potential crystallization at the ambient temperature.¹⁹ In addition, trend line 1 in Figure 12 shows a poor fit than trend line 2, with fitting R^2 factors of 0.981 and 0.988, respectively. Taking into account that the resins investigated by Hosoda¹⁸ were ethylene-1-butene copolymers whose MWs were unclear, our results on average largely agreed with his, albeit the SCB contents in the flat regions were higher than those he reported.

A comparison of SCBD of the analytic- and prep-scale RT solubles of PE-A and PE-B revealed that in the same solvent, the former contained less SCB than did the latter in both cases (Figs. 5 and 6). Depending on molecular weight, the difference was about 10–15 SCB/1000 TC. Although it was unclear what caused this, it was speculated that it might have been a result of (1) differences between PE-A and PE-B in inter-/intra-chain heterogeneity^{20,21} and/or (2) the presence of *in situ* ethyl groups in PE-A, that is, for the same SCB content, ethylene-1-butene copolymer had a higher melting temperature than ethylene-1-hexene copolymer, which might be an indication of the ethyl side chains having the ability to be incorporated into the crystal lattice.^{22–26}

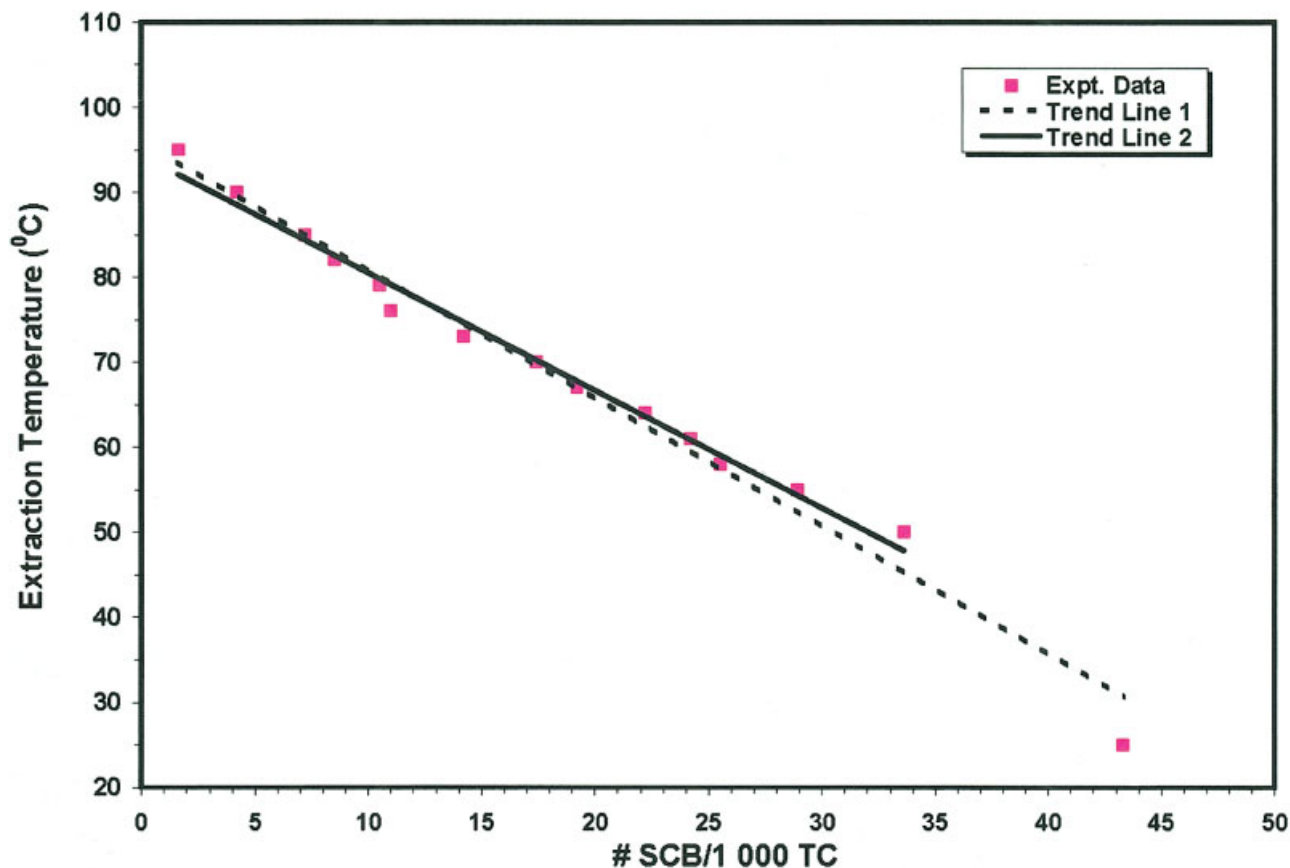


Figure 12 Extraction temperature as a function of SCB content for ethylene-1-butene copolymers (data plotted from Hosoda¹⁸). [Color figure can be viewed in the online issue, which is available at www.interscience.wiley.com.]

Molecular characteristics of lost components of the prep-scale RT solubles

One or more of the following may explain the differences in MW/MWD between the analytic-scale RT solubles and the prep-scale RT solubles. First, they were extracted from different solvents by different procedures. The prep-scale RT solubles went through the precipitation and vacuum-drying processes, but the analytic-scale RT solubles did not. Some low-MW components of the RT solubles may have either not precipitated from the solvent after being poured into the precipitant solvent or been lost during the vacuum-drying process because of their volatile nature. Moreover, the solvents used to extract the prep- and analytic-scale RT solubles were different: TMB for the former, TCB for the latter. The “goodness” of the solvents may play a role in determining the solubility of the highly branched PE chains. Furthermore, the cooling rate and the final temperature at which the RT solubles were extracted were not necessarily the same for the analytic- and prep-scale RT solubles. It was expected that different degrees of cocrystallization could occur under different thermal histories. In a separate experiment, we did observe that the increased extraction temperature resulted in an increased fraction of RT solubles. The experimental re-

sults suggest that the components missing in the prep-scale RT solubles of PE-A were the very low-molecular-weight and branched components.

Unique structural nature of mLLDPE

It is very interesting that PE-C contains an extremely small amount of RT solubles and that the MW/MWD of the RT solubles of PE-C are much smaller than that of PE-A and PE-B. Unlike PE-A and PE-B, the metallocene-catalyzed PE-C had a flat SCBD profile, that is, the SCB was uniformly distributed in the polymer chains regardless of molecular weight (Fig. 1). As a consequence, for resins of the same density, of the three parent resins, metallocene-type LLDPE PE-C consumed the least amount of comonomer (Table I). This is, the mLLDPE used SCB more efficiently to suppress polymer density than did either PE-A and PE-B. With the data listed in Table I, it can be shown that the polymer chains in PE-C had an average run length of about 86 methylene repeating units homogeneously appearing on backbones across the entire MWD. Without heterogeneity in each fraction of the MW of the polymer, it would be possible to attain a melting temperature much higher than RT for the crystals formed [Fig. 10, eq. (3)]. It is this homoge-

neous nature of the SCB distribution on the backbone that resulted in an extremely small fraction of RT solubles in the metallocene-catalyzed PE-C.

In contrast, the total SCB of the RT solubles of PE-A and PE-B was 15.2 and 33.8 wt %, respectively (Table I). Even though PE-A and PE-B had a significantly higher SCB content than did PE-C (Table I), their densities remained higher than that of PE-C. Because most components of RT solubles will end up in the amorphous phase, the SCB in the RT solubles apparently were less effective in suppressing polymer density than that in the semicrystalline phase.

CONCLUSIONS

Room-temperature soluble fractions of a Cr-based LDPE (PE-A), a conventional LLDPE (PE-B), and a metallocene-based mLLDPE (PE-C) were found to have the following molecular characteristics, as studied by SEC, SEC-FTIR, and NMR.

First, the MWD profiles of the RT solubles of these three low-density film resins were significantly different. Although the MWD profile of PE-A was distinctively bimodal, with a sharp peak on the low MW side and a broad peak on the high MW side, that of PE-B appeared to have a single mode with a broad MWD. The cutoff molecular weights for the RT solubles of PE-A and PE-B were approximately 400,000 and >1,000,000 g/mol, respectively. In contrast, the RT solubles of PE-C mainly contained polymer additives and maybe some very-low-molecular-weight (MW < 1000 g/mol) polyethylene molecules. Furthermore, both the amount of RT solubles and the comonomer content of the RT solubles were in the order PE-B > PE-A ≫ PE-C.

Second, the high-molecular-weight components (MW > 10,000 g/mol) of the RT solubles of PE-A and PE-B in general were highly branched components with a homogeneous SCB distribution. However, for the low-molecular-weight components, SCB content was found to be a function of the molecular weight and increased with an increase in molecular weight. When the chain ends were considered as an SCB equivalent, the sum of the SCB and chain-end distribution across the molecular weight distribution was found to be practically flat, suggesting that the driving force for polymers staying in the solution upon cooling to room temperature was the run length of the methylene units, as they were too short to form lamellae with a melting temperature above room temperature, regardless of the molecular weight of the polymer.

Third, even with an SCB content as high as 16 mol %, the SCB in the RT solubles of PE-A and PE-B were superrandomly distributed across the polymer chains. This means that the observed comonomer clusters in the polymer chains of the RT solubles of PE-A and PE-B were lower than would be predicted by Bernoullian statistics, indicating that the addition of a comonomer to

a comonomer-ended propagating chain was hindered presumably by the unfavorable steric energy.

The authors thank the following individuals for their contributions to this study: Ms. Delores Henson for technical assistance with SEC; Mr. Melvin Hildebrand for extracting the prep-scale RT solubles; Dr. Antoni Jurkiewicz for the NMR tests; and Dr. Tim Johnson and Dr. Eric Hsieh for helpful discussions in the early stage of the study. And, finally, we thank Chevron Phillips Chemical Company LP for allowing publication of this work.

References

1. Cipriani, C.; Trishman, A. *Chem Eng* 1982, 89, 66.
2. (a) Arai, K.; Toshimitsu, M.; Tano, A. *Jpn Kokai Tokkyo Koho JP 08,259,632* (1995). (b) Sagar, V. R.; Veraa, M. J.; Trudell, B. C. *PCT WO9724375* (1997).
3. Code of Federal Regulations, Title 21, Vol. 2, 21CFR177.1520.
4. Budke, C. C.; Peat, I. R. *Plastic Eng* 1992, 48, 19.
5. Wild, L. *Adv Polym Sci* 1990, 98, 1.
6. Yau, W. W.; Kirkland, J. J.; Bly, D. D.; *Modern Size Exclusion Chromatography*, Wiley: New York, 1979.
7. Yu, Y.; DesLauriers, P. J.; Rohlfing, D. C. unpublished results.
8. (a) DesLauriers, P. J.; Rohlfing, D. C.; Hsieh, E. T. *Polymer* 2001, 43, 159. (b) DesLauriers, P. J. In *Multiple Detection in Size-Exclusion Chromatography*; Striegel, A. M., Ed.; ACS Symposium Series 893; American Chemical Society: Washington, DC, 2003; Chapter 13.
9. (a) Brereton, R. G. *Chemometrics: Data Analysis for the Laboratory and Chemical Plant*, Wiley: New York, 2003. (b) Beebe, K. R.; Pell, R. J.; Seasholtz, M. B. *Chemometrics: A Practical Guide*; Wiley: New York, 1998.
10. Randall, J. C. *J Macromol Sci Rev Macromol Chem Phys* 1989, C29, 201.
11. Tso, C. C.; DesLauriers, P. J. *Polymer* 2004, 45, 2657.
12. (a) Hsieh, E. T.; Randall, J. C. *Macromolecules* 1982, 15, 1402. (b) Randall, J. C.; Hsieh, E. T. In *NMR and Macromolecules, Sequence, Dynamics, and Domain Structures*; Randall, J. C., Ed.; ACS Symposium Series 247; American Chemical Society: Washington, DC, 1984; p 132.
13. Koenig, J. L. *Chemical Microstructure of Polymer Chains*; Wiley: New York, 1980.
14. Bovey, F. A. *Chain Structure and Conformations of Macromolecules*; Academic Press: New York, 1982.
15. Wunderlich, B. *Macromolecular Physics*; Academic Press: New York, 1980; Vol. 1.
16. Bassett, D. C. *Principles of Polymer Morphology*, Cambridge University Press: London, 1981.
17. Note: The data in Figure 12 were adapted from the Aldrich Chemical Catalog, from which the median melting temperatures of each *n*-alkane were adopted.
18. Hosoda, S. *Polym J* 1988, 20, 383.
19. Shanks, R.; Chen, F.; Amarasinghe, G. *Chin J Polym Sci* 2003, 21, 231.
20. Fu, Q.; Chiu, F.-C.; McCreight, K. W.; Guo, M.; Tseng, W. W.; Cheng, S. Z. D.; Keating, M. Y.; Hsieh, E. T.; DesLauriers, P. J. *J Macromol Sci, Phys* 1997, B36, 41.
21. Hsieh, E. T.; Tso, C. C.; Byers, J. D.; Johnson, T. W.; Fu, Q.; Cheng, S. Z. D. *J Macromol Sci, Phys* 1997, B36, 615.
22. Sanchez, I. C.; Eby, R. K. *Macromolecules* 1975, 8, 638.
23. Helfand, E.; Lauritzen, J. I. *Macromolecules* 1973, 6, 631.
24. Sanchez, I. C. *J Macromol Sci, Rev Macromol Chem* 1974, C10, 113.
25. Mirabella, F. M.; Ford, E. A. *J Polym Sci, Polym Phys* 1987, 25, 777.
26. Kim, M.-H.; Phillips, P. J.; Lin, J. S. *J Polym Sci, Polym Phys* 2000, 38, 154.